Notas de Física - Volume XV - Nº 15

MÖSSBAUER SPECTROSCOPY APPLICATION TO COORDINATION CHEMISTRY *

J. Danon
Centro Brasileiro de Pesquisas Físicas
Rio de Janeiro

(Received August 27, 1969)

There are number of review papers discussing the different aspects of the Mössbauer effect in connection with chemical concepts [1, 2, 3, 4]. In the present chapter we shall take point of view of a coordination chemist who asks to what extent the Mössbauer effect can be of any help for the specific problem of his field.

Coordination chemistry deals with coordination or complex compounds. Such compounds contain a central ion M bounded to several ligands L, L', L", etc. Although complexes can be formed by all electropositive elements M is in most cases a transition metal ion. ** We are in a fortunate position here since one

* Delivered at the Mössbauer Effect Workshop, Catholic University, Washington D.C., 1968.

** An illuminating discussion of the concept of complex compound and its evolution in the development of modern inorganic chemistry is given in Cotton and Wilkinson's book [5].

of the most important transition element is iron, for which we dispose of the Fe^{57}, which is the most favorable for Mössbauer spectroscopy. Besides Fe, Mössbauer investigations have been made with coordination compounds of Ni, Ru, Os, Ir, Pt, Au, Eu and Np among the transition elements, and of Sn, Sb, Te, I, Xe and Kr among the non-transition elements.

Typical problems of coordination chemistry frequently deal with the question of the number and arrangement of the ligands in a complex compound.

To a given stochiometric formula ML'L" etc., we can have a variety of geometrical disposition of the ligands in the coordination sphere. For example, the complex $Co(CN)_5H_2O$ is penta or hexa-coordinated depending if the water molecule is or not bounded to the Co ion (Fig. 1). If this complex is penta-coordinated it can be a trigonal bipyramid or a square pyramid. In any of these geometrical arrangements we may have a complex where all the CN are bounded to the Co though the carbon or some through the N end of the CN ligand, illustrating a case of the so-called ligand isomerism.

Other coordination chemistry problems concern the nature of chemical bonding in the complex. The simplest and at the same time fundamental question is that of the valence state of the central metal ion the complex. A further step is to consider the electronic strucutre of the central ion taking into account the perturbation introduced by the electric field from the ligands. The aim of this ligand field approach is to

determine the electronic wave function for the ground state of the central ion. In a more elaborate approach, such as that of the molecular orbital theory, the purpose is to establish the energy levels and the charge distribution at the central ion and at the ligands of the complex ion.

A common feature to all spectroscopic methods is that they can be used in two ways: on the basis of selection rules and symmetry arguments and on the basis of a detailed analysis envolving the electronic structure of the molecule. Using the first procedure we derive information on molecular architecture, valency states, nature of the ligands, etc., without any detailed theoretical analysis regarding the molecule. Typical examples are given by infra-red and Raman spectroscopies from which practically all information is obtained through the assignement of the absorption bands which are classified according to selection rules and symmetry arguments. However it is also possible to make a detailed analysis of force constants on the basis of the electronic structure of the molecule. On the other hand in a spectroscopic method such as electron spin resonance the interpretation of most spectra requires the location of the unpaired electron in a given electronic energy level. For this reason in this spectroscopic method the information is mainly derived from the analysis of the electronic structure of the molecule.

The Mössbauer spectroscopy has also this dual character.

The hyperfine interactions on which is based the Mössbauer spectroscopy are subject to selection rules and symmetry arguments. The basic selection rule assigns distinct ranges of values of the isomer shift for different oxidation states of an element. Using this selection rule we are able to classify the complex compounds of an element according to the oxidation state of the central ion. The other hyperfine interaction, such as the quadrupole coupling and the magnetic splitting are also a function of the oxidation state of the element, but in a less general way as compared to the isomer shift. Fig. 2 illustrates the use of the isomer shift selection rule in ruthenium coordination chemistry [6].

The basic symmetry argument of Mössbauer spectroscopy envolves the nuclear quadrupole coupling and states the absence of quadrupole splitting when the surroundings of the nucleus have cubic symmetry. By this symmetry arguments we can say if the molecular geometry around an element is or not distorted from octahedral symmetry. Moreover the value of the quadrupole coupling is sensitive to the symmetry of the electronic distribution around the nucleus. Thus in the case of iron the range of values quadrupole coupling are distinct for the different spin configurations of a given oxidation state. On this basis it is frequently possible to decide between the high or low-spin configuration for the iron ion in its complex compounds.

We shall now illustrate the uses of Mössbauer spectroscopy to coordination chemistry based on these selection rules and symmetry arguments, deriving all information from the shape and position of the Mössbauer spectra.

CRYSTALLINE STRUCTURE

Information which as similar or complementar to that derived from X-ray diffraction can be obtained from Mössbauer spectroscopy. A typical example is the Mössbauer evidence of inequivalent ferrous ions in ferrous formate [7]. The spectra of the polycrystalline complex consists of four sharp peaks (fig. 3). This pattern has been attributed to two quadrupole splittings arising from different effective electric field gradients corresponding to two inequivalent ferrous ions sites. Fig. 4 shows the nearest neighbour symmetry of the two sites: one is O_h and the other D_{4h}.

COMPLEX ISOMERISM

Compounds with the same stoechiometric composition but different arrangement of the ligands are called isomers. The Mössbauer spectrum may be of great help for deciding the different possibilities for the structure of an isomer.

The common hydrated ferric chloride, $FeCl_3.6H_2O$, was long time assumed to have the iron ion surrounded by an octahedral environement of water molecules as shown in fig. 5. The Mössbauer spectrum of this molecule [8] exibits a large quadrupole

splitting and on the basis of this result it was suggested that the symmetry around the ferric ion should be lower than octahedral. This was the starting point of X-ray diffraction investigations [9] which have shown that the correct structure is that of an hydrated isomer, as in illustrated in fig. 6. This result is of interest for understanding the properties of aqueous solutions of the ferric ion in the presence of chloride ions, since the different complexes which are formed are derived from this basic distorted structure [10].

CIS-TRANS ISOMERISM

This frequent case of isomerism is illustrated in fig. 7.

The differences in ligand disposition should induce different values of the electric field gradient at the central ion: in the trans-case there is axial symmetry (D_{4h}), which is absent in the cis-case (C_{2v}). In a treatment based on a point-charge model the field gradient is given by:

$$q = (1 - \gamma_\infty) \left\{ \sum_i q_i (3 \cos^2 \theta_i - 1) / r_i^3 \right\}$$

where $(1 - \gamma_\infty)$ corrects for anti-shieding effects, q_i is the magnitude of the i-th charge, whose coordinates are r_i and θ_i. Since $\theta = 0$ for the trans-case and $\theta = \pi/2$ for the cis-case, as is illustrated in fig. 8, one finds the ratio of quadrupole

splitting

$$\frac{\Delta E_{trans}}{\Delta E_{cis}} = 2:1$$

Table 1 lists the results obtained [11] in a series of low-spin cis-trans isomers of iron (II).

Within the experimental error the ratio 2:1 is observed. The results suggest that the cis-trans isomerism reported for dicyanobis (1,10 phenantroline) iron (II) is doubtfull.

One can identify by this simple procedure which is the cis and which is the trans isomer.

LIGAND LINKAGE ISOMERISM

Coordination chemists have been recently interested in the problem of the isomerism of the cyanide ligand. The carbon end of the cyanide ligand creates a strong field and tends to form low-spin complexes whereas the nitrogen end is a weak field ligand and usually gives high-spin complexes.

The X-ray structure of the metal ferrocyanides, like the Prussian blue and similar compounds, shows that one metal is bounded to the nitrogen and the other carbon, as is illustrated in fig. 9. The phenomena of cyanide likage isomerism has been investigated [12] in iron (II) hexacyano-chromate (III).

This complex with composition $Fe_3^{II}|Cr^{III}(CN)_6|$

exhibits the linkage isomerism: at room temperature it changes spontaneously from form I to form II, as illustrated in fig. 10.

According to the arguments previously discussed concerning the difference of strength of the ligand field induced by both ends of the CN ligand, one should expect a high-spin complex of Fe^{+2} in form I and a low-spin iron (II) complex in form II. The Mössbauer spectra of the form I shows indeed the typical isomer shift and quadrupole splitting of high-spin Fe^{+2}. As the spontaneous isomeration process leads to form II the quadrupole coupling decreases, going to the range of low values characteristic of the ferrous ion in the low-spin configuration.

SPIN-STATE EQUILIBRIA

Magnetic susceptibility measurements have suggested the coexistence at a given temperature of different spin configurations of a transition ion in a same complex. A conclusive evidence of this fact has been obtained from the study of the changes of the Mössbauer spectrum of Iron (II) - Bis - (1,10 phenantroline) complex as a function of temperature [13]. The results are listed in Table II. These results show a variation of the hyperfine parameters from the range of values of high-spin to low-spin configuration of the ferrous ion.

This data provides evidence for the existence of spin-

state equilibria between the almost equi-energetic $^5T_2$ and $^1A_1$ states. As a matter of fact this is the first reported quintet-singlet equilibrium in a transition metal complex.

STRUCTURE OF COMPLICATED COMPLEX COMPOUNDS

The earliest recorded coordination compound is Prussian blue, obtained by Diesback during the first decade of the 18th century. Since its discovery the structure of this compound has been object of much discussion. In the 1930 edition of the Gmelins Handbuch der Anorganischen Chemie, in the volume of iron, more than a thousand pages are devoted to the properties of this and related complexes.

The main question regarding the Prussian blue, both in the soluble and insoluble form, and the Turnbull blue are:
1) Which are the electronic configurations of the two kinds of iron in these compounds: ferric ferrocyanide, $Fe^{III}|Fe^{II}(CN)_6|$ ferrous ferricyanide $Fe^{II}|Fe^{III}(CN)_6|$ or more complex configuration ?

2) Whether Prussian blue, which is made by mixing the solutions of ferric compound and ferrocyanide ion and Turnbull's blue, which is made by mixing the solutions of ferrous compound and ferrocyanide ion are the same compound or not ?

We found the answer of the questions which have been the object of so many discussions in a recent report by A. Ito, M. Suenaga and K. Ono [14], "Mössbauer Study of Soluble Prussian Blue, Insoluble Prussian Blue and Turnbull's Blue" in 13 pages.

The Mössbauer spectra were observed in the range 1.6 to 300°K. At the lowest temperature the spectra we well resolved and show a superposition of hyperfine split levels and a single line for all the compounds, as is illustrated in fig. 11.

The results obtained are listed in tables 3 and 5 and compared with typical values of Mössbauer parameters for the various states of iron (table 4).

By comparing the internal field for the two kinds of iron ions with typical values it is seen that H_i = 540 kOe is just the value of high-spin Fe^{+3} and the of H_i = 0 kOe corresponds to low-spin Fe^{+2}. The isomer shift and the quadrupole splitting for each iron species are also consistent with typical values for Fe^{+3} and Fe^{II} respectively.

One concludes that iron has in the compounds definite electronic states which are Fe^{+3} ionic and covalent Fe^{II}. Valence oscillation or resonance between structures.

$$Fe^{II}(CN)_6Fe^{+3} \longleftrightarrow Fe^{III}(CN)_6Fe^{+2}$$

does not occur at 1.6 K°, or at least occursmuch more rapidly than 10^{-8} sec (time of Larmor precession of the Fe^{57} nucleus).

Since the spectra of soluble Prussian blue, insoluble Prussian blue and Turnbull's blue give almost the same values for the hyperfine interactions we conclude that the electronic structure of these compounds are the same from a Mössbauer

spectra point of view. Therefore, in Turnbull's blue, which is made by ferrous compounds and ferricyanide, the charge transfer from Fe^{+2} with high-spin to Fe^{III} with low-spin or flipping of the CN ligand by 180° should occur at the instant of a combination.

The intensity ratios of the Mössbauer spectra are consistent with the stoichiometric formula $KFe|Fe(CN)_6|$ for soluble Prussian Blue, $Fe_4|Fe(CN)_6|$ for insoluble Prussian blue and Turnbull's blue. Thus, from the comparison of the Mössbauer spectra we obtain all the basic information on the structure of these complicated complexes.

ELECTRONIC STRUCTURE OF MOLECULES

Let us now exemplify the use of Mössbauer spectroscopy for obtaining information on the electronic structure of molecules. As was mentioned earlier, a theoretical model is now required in order to interpret the results.

a) Using ligand field theory

Ligand field theory has been used for interpreting the large quadrupole splitting observed in high-spin ferrous compounds, which are temperature dependent and vary markedly from compound to compound fig. 12 [15]. In the ferrous ion the $3d^6$ of electrons are distributed in the high-spin configuration with maximum multiplicity along the five d orbitals. As is shown in fig. 13, this configuration leads to an extra

electron with the spin antiparallel to the other five.

The main contribution to the field gradient at the iron nucleus is given by this extra electron. Since the configuration of five parallel spins results in spherical symmetry, their electronic contribution to the electric field gradient at the nucleus vanishes. The values of the electric field gradient produced by the different 3d wave functions in the presence of the crystal field are listed in table 6.

The orbital in which the extra electron will be placed depends on the deviation from cubic symmetry of the ligand field. As is illustrated in fig. 14, axial and rhombic fields lift the degeneracy within the d_γ and d_ϵ shells and further splitting of the energy levels occurs by spin-orbit coupling. The temperature dependence of the quadrupole splitting is due to the distribution of the electron among these sub-levels. Covalency effects are introduced by considering that the bonding delocalizes the 3d electron. A covalency coefficient $\alpha^2 < 1$ accounts for the expansion of the radial part of the 3d wave function. Using this treatment it has been possible to obtain reasonable estimates of the energy splitting of the ligand field and covalency parameters (table 7) by an adequate choice of the ground state wave function in order to fit the temperature dependence of the quadrupole splitting showed in fig. 12.

b) Using molecular orbital theory

The use of molecular orbitals for interpreting the Mossbauer hyperfine parameters has been demonstrated in the case of the nitroprusside complex [16], $Fe^{II}(CN)_5NO^{2-}$.

The M. O. level scheme proposed for this complex is reproduced in fig. 15. The Φ wave functions can be regarded as the antibonding combinations which would be formed with a symmetric octahedron of CN ligands. They are perturbed by the ligand field distortion arising from the substitution for one of the CN's by NO. The π^* and σ^* orbitals of NO overlap with the central ion wave functions, forming relative bonding and antibonding combinations. ψ_{xy} and all levels below are filled with paired electrons. However, the electron delocalization will be different in these orbitals since ψ_{xy} is essentially non-bonding whereas the lower doublet (ψ_{xz}, ψ_{yz}) forms strong π^* antibonds with the empty orbitals of NO. These three full levels give rise to assymmetrical charge distributions and induce a electric field gradient at the iron nucleus which can be written as:

$$q = \left\{ \frac{4}{7} n_{xy}^2 - \frac{2}{7} (n_{xz}^2 + n_{yz}^2) \right\} \langle r^{-3} \rangle \qquad (1)$$

where the n^2 are the effective d electron population in the corresponding M.O.

The quadrupole splitting of 3.60 mm/sec in a high spin

Fe^{+2} complex, such as $FeSiF_6.6H_2O$, is due to a single 3d electron with field gradient:

$$q = \frac{4}{7} n^2 \langle r^{-3} \rangle$$

with $n^2 = 0.80$.

Taking the ratio of quadrupole splittings as the ratio of field gradients one has:

$$\frac{\Delta E}{3.60} = \frac{\frac{4}{7} n_{xy}^2 - \frac{2}{7}\left(n_{xz}^2 + n_{yz}^2\right)}{\frac{4}{7} \times 0.8} \quad . \qquad (2)$$

Using the calculated values [17] $n_{xy}^2 = 2(0.81)$ and $n_{xz}^2 = n_{yz}^2 = 2(0.61)$ one finds 1.8 mm/sec., which is in good agreement with the experimental quadrupole splitting of 1.726 mm/sec reported for sodium nitroprusside.

This results confirms the strong delocalization of the d_{xz}, d_{yz} iron electrons in the pentacyanonitrosyls, showing the basic importance of back-donation in determining the energy levels of these molecules.

c) Using the spin-hamiltonian

Abragam and Pryce [18] have developed a perturbation procedure for the calculation of splittings of a paramagnetic ion which has found extensive application in electron spin resonance studies [19]. This method, which employs the so-called spin-hamiltonian, has been used for interpreting Möss-

bauer spectra of paramagnetic complex ions [20, 21]. We will not give a complete discussion of the spin Hamiltonian for which the reader is refered to specialized references, but rather outline the use of this method in Mössbauer spectroscopy.

A general spin-hamiltonian is the sum of energy operators:

$$\begin{aligned}\mathcal{H} = {} & \beta(g_z H_z S_z + g_x H_x S_x + g_y H_y S_y) \\ & + D\left\{S_z^2 - 1/3S(S+1)\right\} + E(S_x^2 - S_y^2) \\ & + A_z S_z I_z + A_x S_x I_x + A_y S_y I_y \\ & + P\left\{I_z^2 - 1/3I(I+1)\right\} + P'(I_x^2 - I_y^2) \\ & + g_n \beta_N \, H.I\end{aligned} \qquad (3)$$

H is the external magnetic field and S is the "effective spin" of the paramagnetic ion, such that 2S + 1 is the multiplicity of the lowest group of electronic states. In simple cases S is equal to the ionic spin.

The first line represents the interaction of the effective spin with the external field, whereas the last line represents the interaction of this field with the nuclear spin. β is the Bohr magneton and β_N the nuclear magneton.

The second line expresses the coupling of electron orbitals to the lattice. D and E are related to the electrostatic ligand field.

The third line expresses the coupling between the effective spin of the electrons and the nuclear spin.

The fourth line expresses the quadrupole coupling of the nucleus.

Let us see now how the spin-hamiltonian is used for the study of an iron complex of biological importance.

The azide derivative of haemoglobin (fig. 16) contains a low-spin ferric ion (S = 1/2) with a single hole in the lower orbital triplet. From electron spin resonance measurements [22] it was found $g_x = 1.70$, $g_y = 2.20$ and $g_z = 2.82$.

The spin-hamiltonian for an effective spin S = 1/2 reduces to the first line of (3) since the second term vanishes, and the remaining ones are dropped because the hyper fine structure is not resolved in most electron spin resonance spectra of iron compounds.

Using the spin-hamiltonian

$\mathcal{H} = \beta (g_z H_z S_z + g_x H_x S_x + g_y H_y S_y)$ with the ground state wave function for the iron ion:

$$\psi^+ = a|1\alpha\rangle + b|\xi\beta\rangle + c|-1\alpha\rangle$$
$$\psi^- = a|-1\beta\rangle - b|\xi\alpha\rangle + c|1\beta\rangle \qquad (4)$$

where $|1\alpha\rangle$, $|\xi\beta$, etc. are linear combinations of the d_{xy}, d_{xz} and d_{yz} orbitals, Griffith [23] has established relations between the g values and the wave function amplitudes a, b and c. He fitts the experimental g's with a = 0.841, b = 0.099

and c = 0.532.

The Mössbauer spectrum in the paramagnetic complex results from transition between excited and ground nuclear eigenstates determined by the nuclear spin-hamiltonians. In order to derive the form of these hamiltonians from (3) we observe that the first and last term vanish since we have no external magnetic field. The second line vanishes for the effective spin S = 1/2, and there remain the hyperfine term and the quadrupole coupling one:

$$\begin{aligned}\mathcal{H} &= A_z S_z I_z + A_x S_x I_x + A_y S_y I_y \\ &+ QV_{zz}/4 \left\{ I_z^2 - 5/4 + \eta/3 (I_x^2 - I_y^2) \right\}\end{aligned} \tag{5}$$

In the nuclear ground state the quadrupole couplings vanishes and we have

$$\mathcal{H} = A_z S_z I_z + A'_x S_x I_x + A'_y S_y I_y \tag{6}$$

where the dot is used to differenciate the ground from the excited nuclear state.

Using the wave functions (4) it is possible to express the A's. q and η as a function of a, b and c. [20] Introducing numerical values of the parameters in (5) and (6) and calculating the corresponding eigenstates the line absorption spectrum shown in fig. 17 is obtained which fits satisfactory the observed Mössbauer spectrum [20].

TABLE I

Mössbauer hyperfine parameters of Iron (II) - bis (1,10 phenantroline)

T(^{o}K)	ΔE (mm/sec)	I.S. (mm/sec)
293	2.67 $\pm$ 0.03	0.18 $\pm$ 0.03
77	0.34 $\pm$ 0.06	0.37 $\pm$ 0.05

TABLE II

Mössbauer hyperfine parameters of cis-trans isomers

		ΔE(mm/sec^{-1})	I.S.(mm/sec^{-1})
1.	$\|Fe(CNMe)_6\|(HSO_4)$	0.00	- 0.02
2.	cis-$Fe(CNMe)_4(CN)_2$	0.24	0.00
3.	trans-$Fe(CNMe)_4(CN)_2$	0.44	0.00
4.	$\|Fe(CNEt)_6(ClO_4)_2$	0.00	0.00
5.	$\|Fe(CN)(CNEt)_5\|(ClO_4)$	0.17	+ 0.04
6.	cis-$Fe(CNEt)_4(CN)_2$	0.29	+ 0.05
7.	trans-$Fe(CNEt)_4(CN)_2$	0.59	+ 0.05
8.	$\|Fe(CNCH_2Ph_6\|(ClO_4)_2$	0.00	- 0.04
9.	$Fe(CN)(CNCH_2)Ph)_5ClO_4$	0.28	- 0.02
10.	trans-$\|Fe(CN)_2(CNCH_2Ph)_4\|$	0.56	- 0.01
11.	cis-$Fe(phen)_2(CN)_2$	0.58	+ 0.27
12.	"trans" - $Fe(phen)_2(CN)_2$	0.60	+ 0.33

Errors for I.S. and $\Delta E = \pm 0.05$ mm/sec^{-1}; I.S. values are relative to stainless steel

TABLE III: The obtained values of parameters δ, $(S_1 - S_2)$, and H_{int}. δ is the isomer shift relative to stainless steel, S_1 and S_2 are shown in the figure and $(S_1 - S_2)$ is $1/2\ e^2 q\ Q\ (3\cos^2\theta - 1)$, and H_{int} is the internal magnetic field.

	Soluble Prussian blue		insoluble Prussian blue		Turnbull's blue	
	Fe^{3+}	Fe^{II}	Fe^{3+}	Fe^{II}	Fe^{3+}	Fe^{II}
δ (mm/sec)	0.66±0.05	0.15±0.05	0.66±0.05	0.13±0.05	0.65±0.05	0.09±0.05
$S_1 - S_2$ (mm/sec)	0.37±0.15	0	0.48±0.15	0	0.52±0.15	0
H_{int} (kOe)	536 ± 20	0 ± 10	541 ± 20	0 ± 10	543 ± 20	0 ± 10

TABLE IV: The typical values of parameters δ, ΔE, and H_{int} for various charge state of irons. δ is the isomer shift relative to stainless steel, ΔE is the quarrupole splitting and H_{int} is the internal magnetic field.

	Fe^{3+}(ionic)	Fe^{2+}(ionic)	Fe^{III}(CN)	Fe^{II}(CN)
δ (mm/sec)	~0.5	~1.4	~0	~0
ΔE (mm/sec)	~0.5	1.0~3.4	$\leqslant$ 1.0	~0
H_{int} (kOe)	500~600	0~300	170~270[7]	0

7) The internal magnetic field of low spin Fe^{III} combined with $(CN)_6$ has not been reported. The values in this table were recently obtained for $K_3Fe(CN)_6$[8] and $M_3[Fe(CN)_6]_2$ (M: Mn, Co, Ni, Cu)[9] by us.

8) K.Ôno et al: to be published.

9) M. Suenaga, A. Ito and K. Ôno: to be published.

TABLE V: The intensity ratio between the two kinds of irons Fe^{3+} and Fe^{II}.

	Fe^{3+}/Fe^{II} (observed)(a)	Fe^{3+} / Fe^{II} (normalized)(b)
soluble Prussian blue	1.39	1.00
insoluble Prussian blue	1.78	1.28
Turnbull's blue	1.84	1.32

(a) Fe^{3+}/Fe^{II} observed with the absorbers containing Fe of about 20 mg/cm^2.

(b) that normalized to the thin absorber.

TABLE VI

Values of field gradient q and asymmetry parameter η for 3d electrons

	Orbital	q	η
d_γ	$d_{x^2-y^2}$	$+ 4/7 \langle r^{-3} \rangle$	0
	d_{z^2}	$- 4/7 \langle r^{-3} \rangle$	0
d_ϵ	d_{xy}	$+ 4/7 \langle r^{-3} \rangle$	0
	d_{xz}	$- 2/7 \langle r^{-3} \rangle$	+ 3
	d_{yz}	$- 2/7 \langle r^{-3} \rangle$	- 3

TABLE VII

Covalency-Factors α, Splitting Parameters Δ, and Ground-State Wave Functions Used in Describing the ^{57}Fe Quadrupole Splitting in Several Ferrous Compounds

Compound	α	Δ_1	Δ_2	Ground-State orbital wave function
$FeSiF_6 \cdot 6H_2O$	0.80	760	760	$\|3z^2 - r^2\rangle$
$FeSO_4 \cdot 7H_2O$	0.80	480	1300	$\|xy\rangle$
$Fe(NH_4SO_4)_2 \cdot 6H_2O$	0.80	240	320	$\|xy\rangle$
$FeC_2O_4 \cdot 2H_2O$	0.80	100	960	$\|xy\rangle$
$FeSO_4$	0.80	360	1680	$\|x^2 - y^2\rangle + 0.09\|3z^2 - r^2\rangle$
$FeCl_2 \cdot 4H_2O$	0.80	750	2900	$\|x^2 - y^2\rangle + 0.01\|3z^2 - r^2\rangle$
FeF_2	0.67	1000	2200	$\|x^2 - y^2\rangle + 0.14\|3z^2 - r^2\rangle$

FIGURE CAPTIONS

Fig. 1: Hexa and penta coordinated structures for complex cobal (II) cyanide.

Fig. 2: Graphical representation of the isomer shifts obtained for various ruthenium compounds.

Fig. 3: Mössbauer spectrum taked at liquid helium temperature. The four peaks are labeled a,b,c, and d.

Fig. 4: Schematic diagram of the approximate nearest neighbor symmetry at the two ferrous-ion sites.

Fig. 5: Model of the $Fe(H_2O)_6$ ion with octahedral structure.

Fig. 6: Model of the $|FeCl_2(H_2O)_4|^+$ ion.

Fig. 7: Cis and tans-isomers for the octahedral structures of $Co(NH_3)_4Cl_2$.

Fig. 8: The electric field gradient in a point charge model for cis and trans-isomers.

Fig. 9: The structure of $K_2NiFe(CN)_6$.

Fig. 10: Ligand linkage isomers in iron hexacyanochromate.

Fig. 11: The Mössbauer spectra obtained at 1,6°K for: a) soluble Prussian blue; b) insoluble Prussian blue; c) Trunbull's blue. The line positions for the two kinds of iron are indicated in d) with solid lines and dashed line.

Fig. 12: Quadrupole splitting of several ferrous compounds as a function of the temperature.

Fig. 13: Spin configuration of the 3d electrons of ferrous ion in the high-spin case.

Fig. 14: Energy level scheme for the ferrous ion under the action of the crystalline field plus spin-orbit coupling.

Fig. 15: Energy level diagram for the nitroprusside ion.

Fig. 16: The structure and the three principal axes of g-value variation for myoglobin and haemoglobin azide.

Fig. 17: Comparison of predicted absorption lines and the 1,2° K haemoglobin azide data. The breath of the observed absorption line is attributed to spin relaxation.

* * *

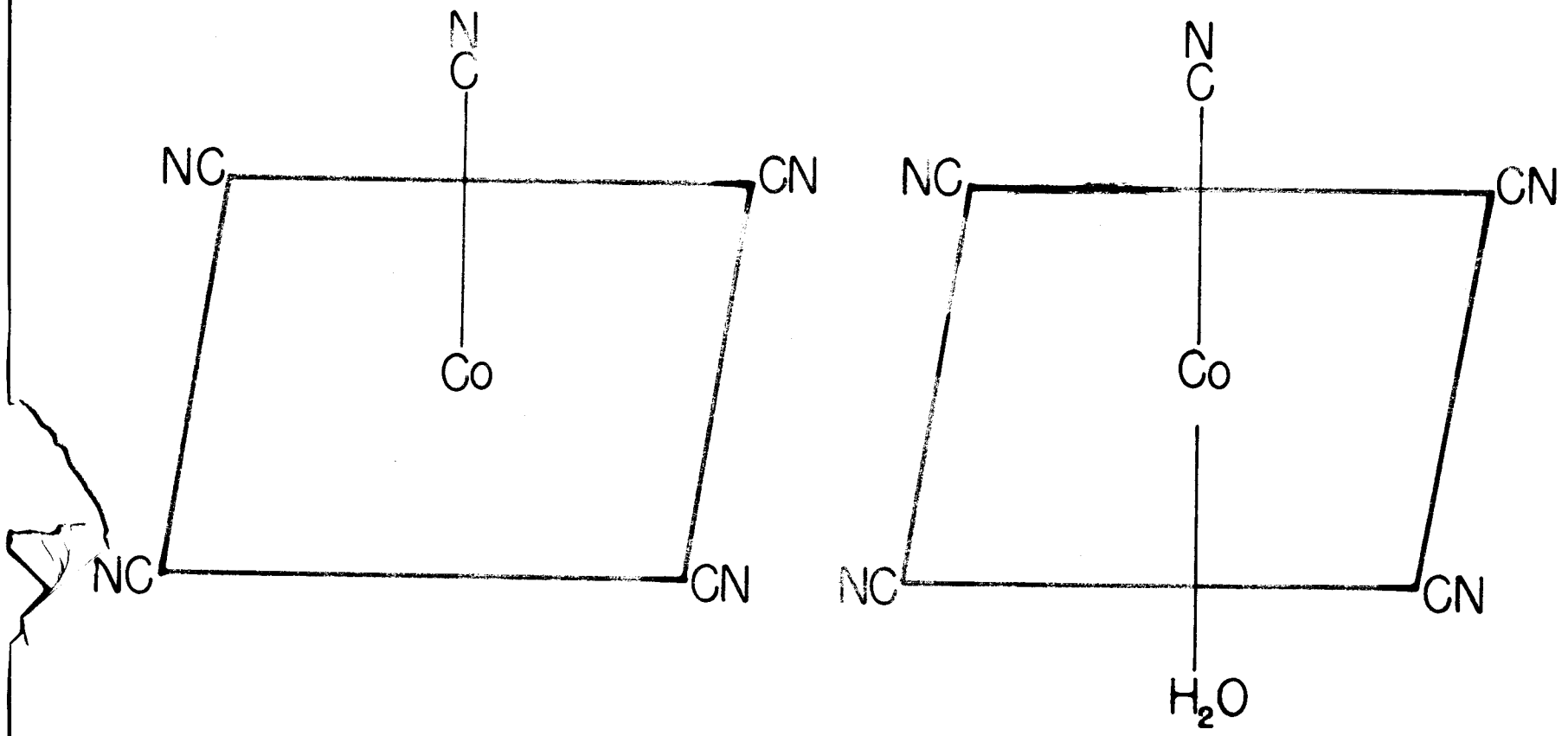

FIG. 1

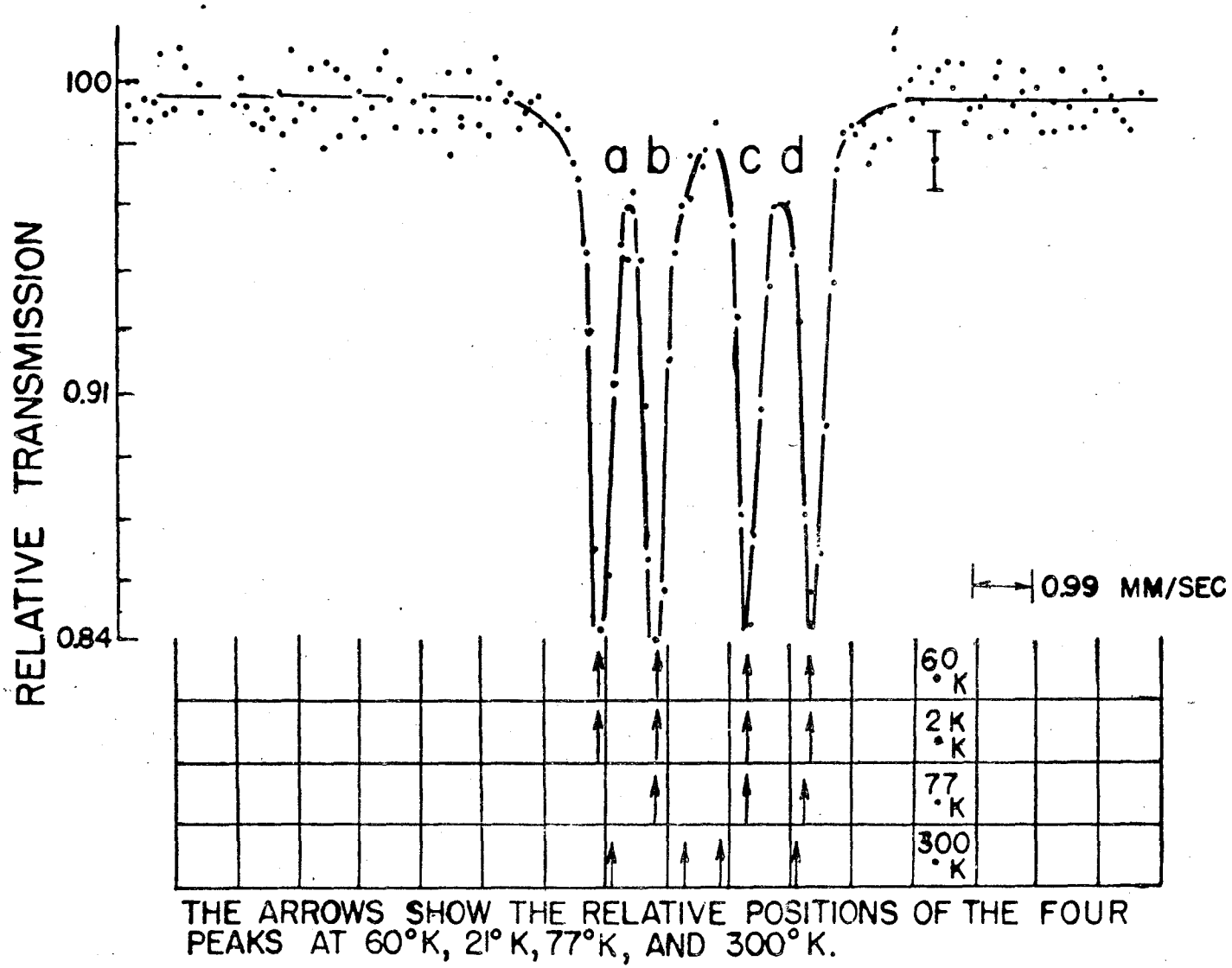

MÖSSBAUER SPECTRUM TAKEN WITH LIQUID HELIUM IN THE DEWAR. THE FOUR PEAKS ARE LABELED a, b, c, and d.

FIG. 3

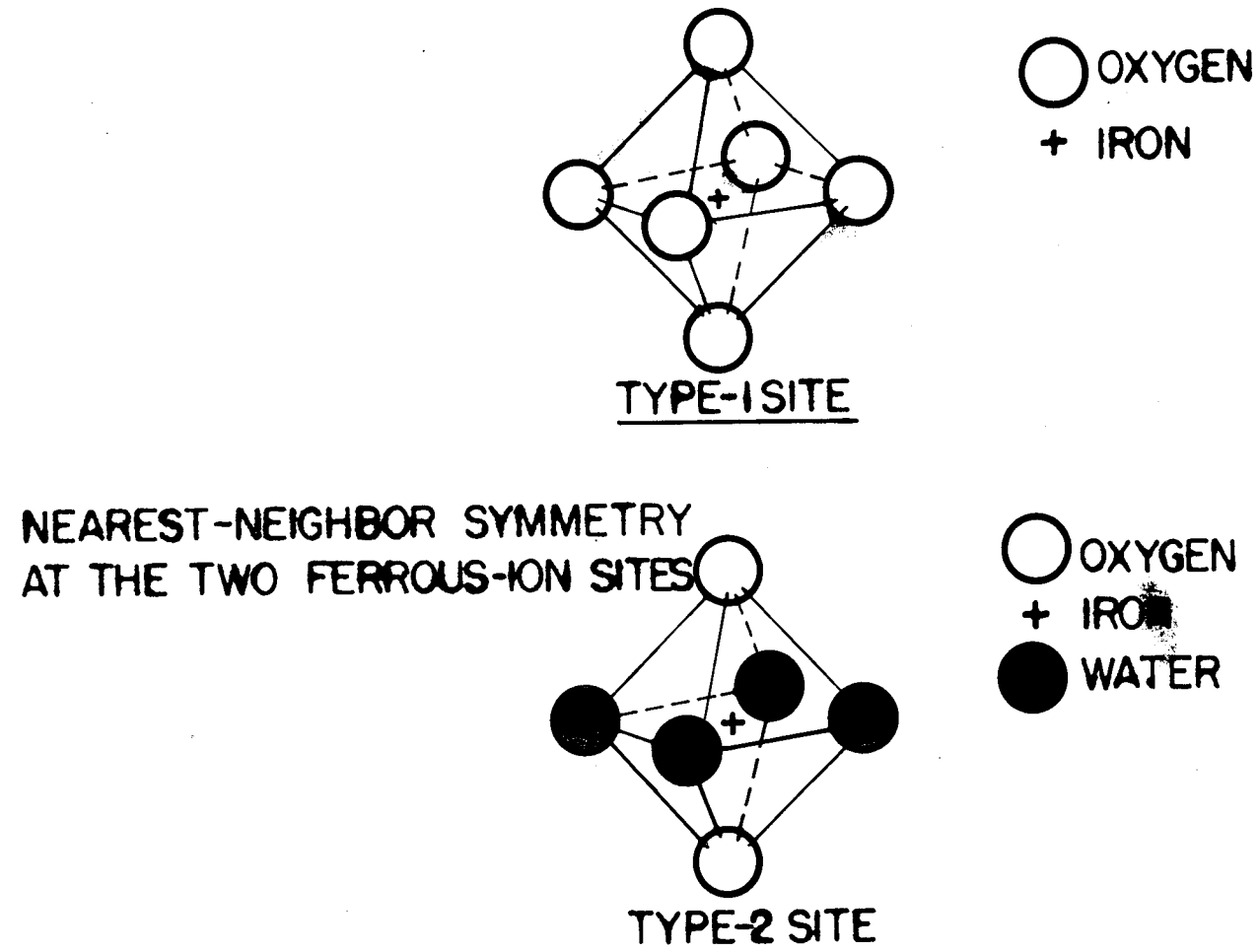
OXYGEN
IRON
TYPE-1 SITE
NEAREST-NEIGHBOR SYMMETRY
AT THE TWO FERROUS-ION SITES
OXYGEN
IRON
WATER
TYPE-2 SITE

FIG. 4

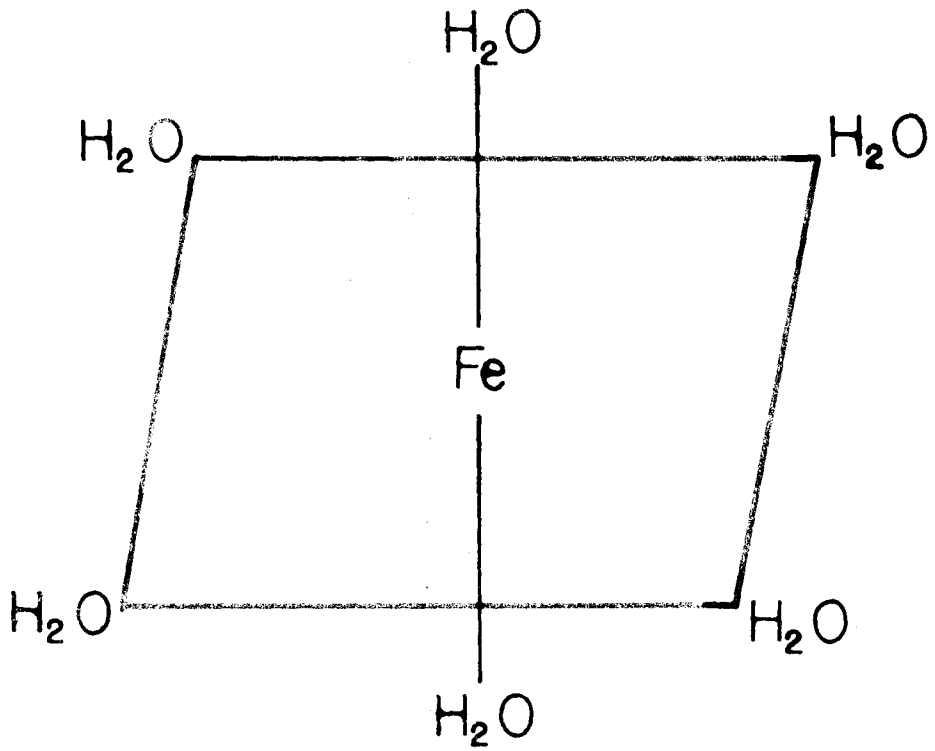

FIG. 5

FIG. 6

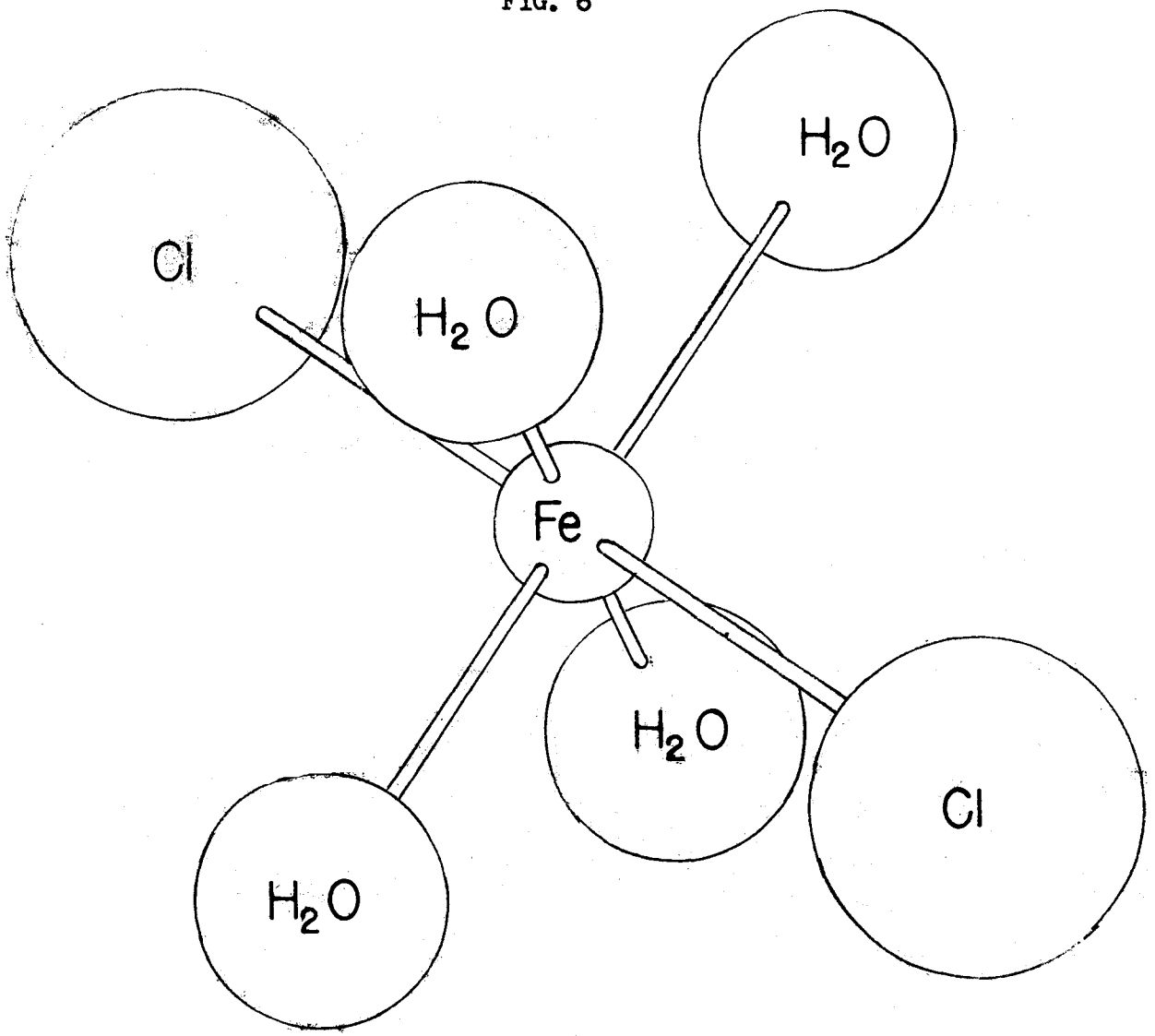

Model of the $[FeCl_2(OH_2)_4]^+$ ion in the crystals its symmetry is C_{2h} -2/m but the deviations from D_{4h} -4/mmm symmetry are small, therefore, the latter symmetry is likely in solutions.

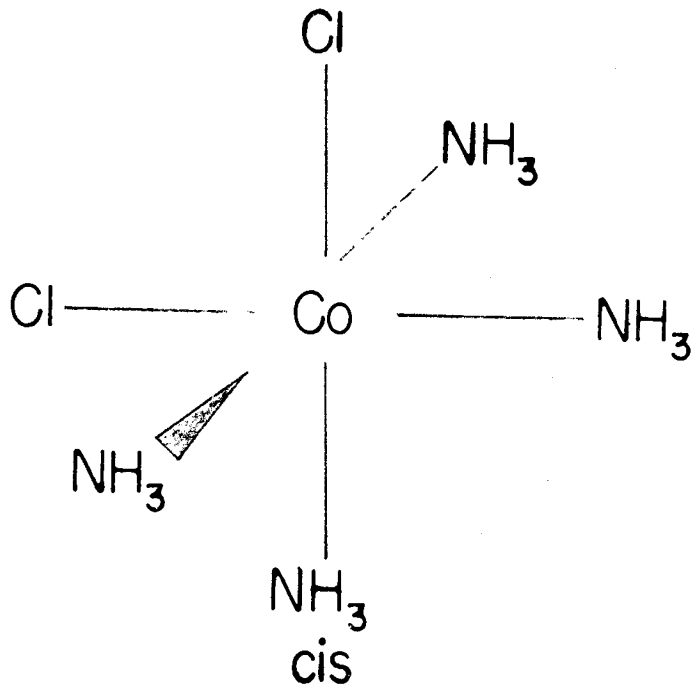

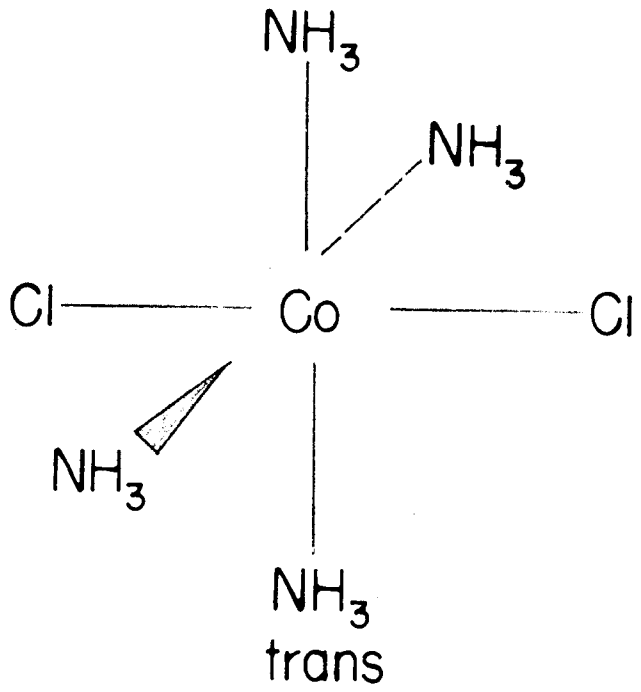

FIG. 7

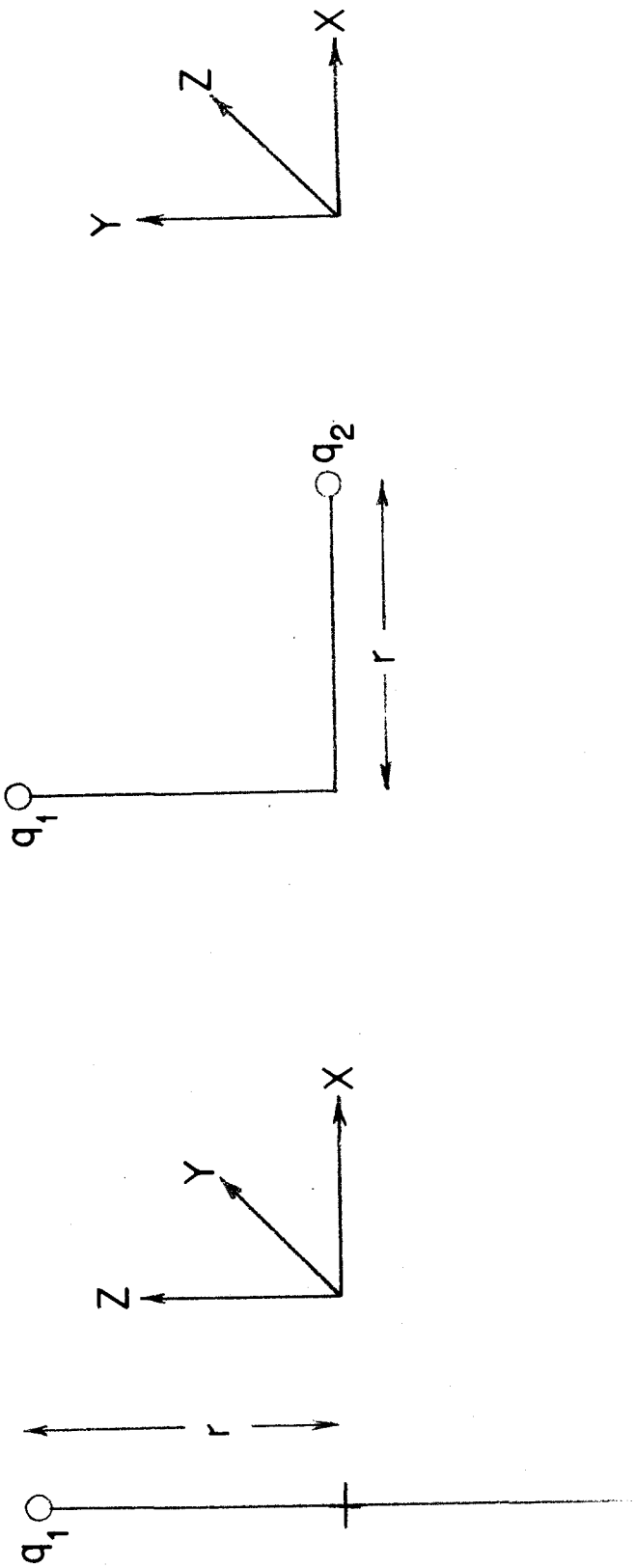
X
Z
Y
q_2
r
q_1
X
Y
Z
r
q_1

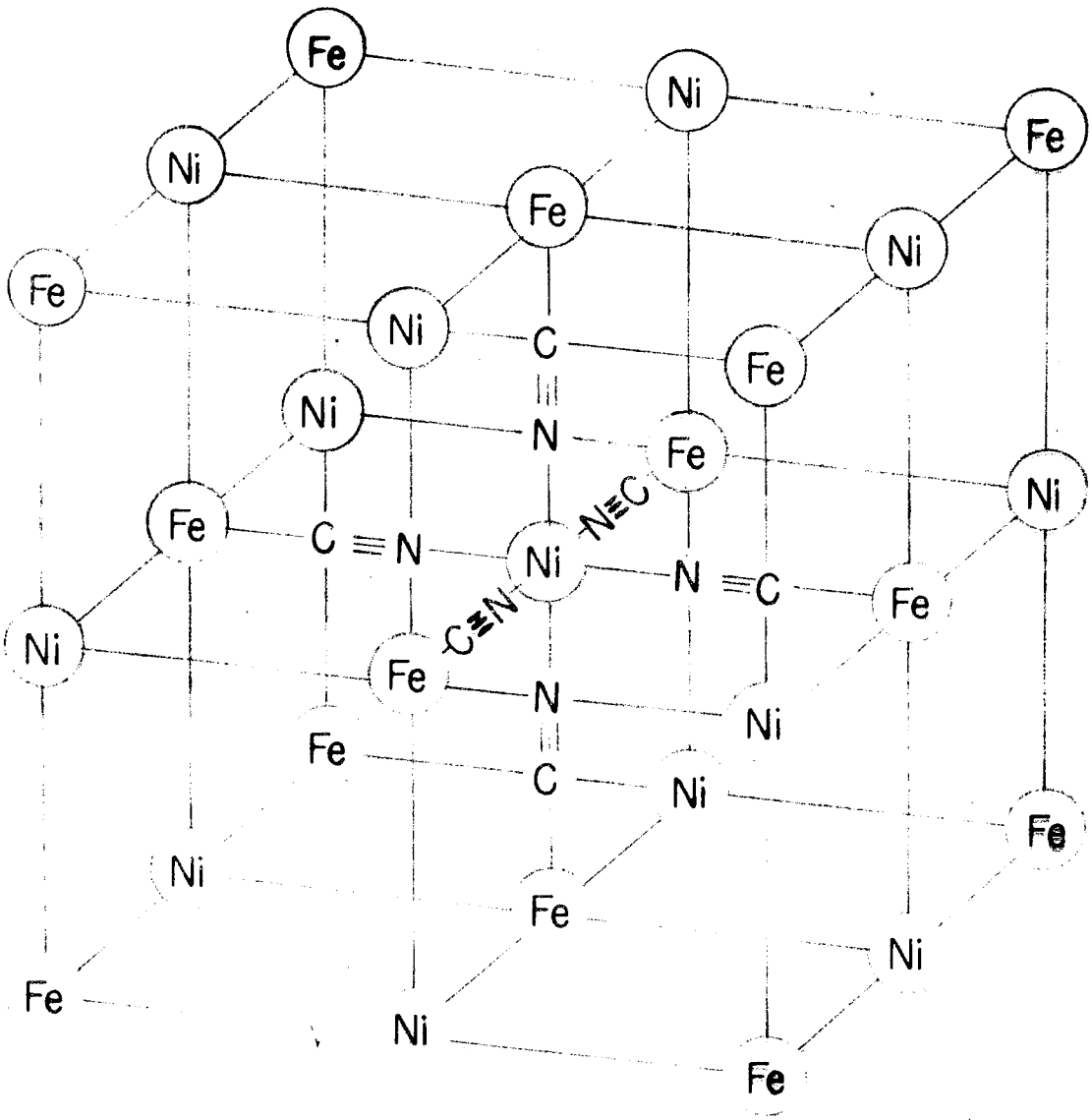
Fe
Ni
Fe
Ni
Fe
Ni
Fe
Ni
C
Fe
Ni
N
Fe
Ni
Fe
C ≡ N
Ni
N ≡ C
Fe
Ni
C≡N
N≡C
Fe
N
Ni
Fe
C
Ni
Fe
Ni
Fe
Ni
Fe
Ni
Fe

FIG. 9

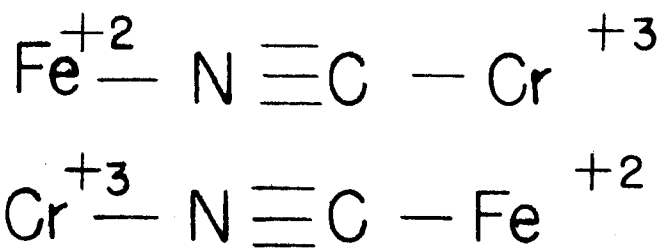

FIG. 10

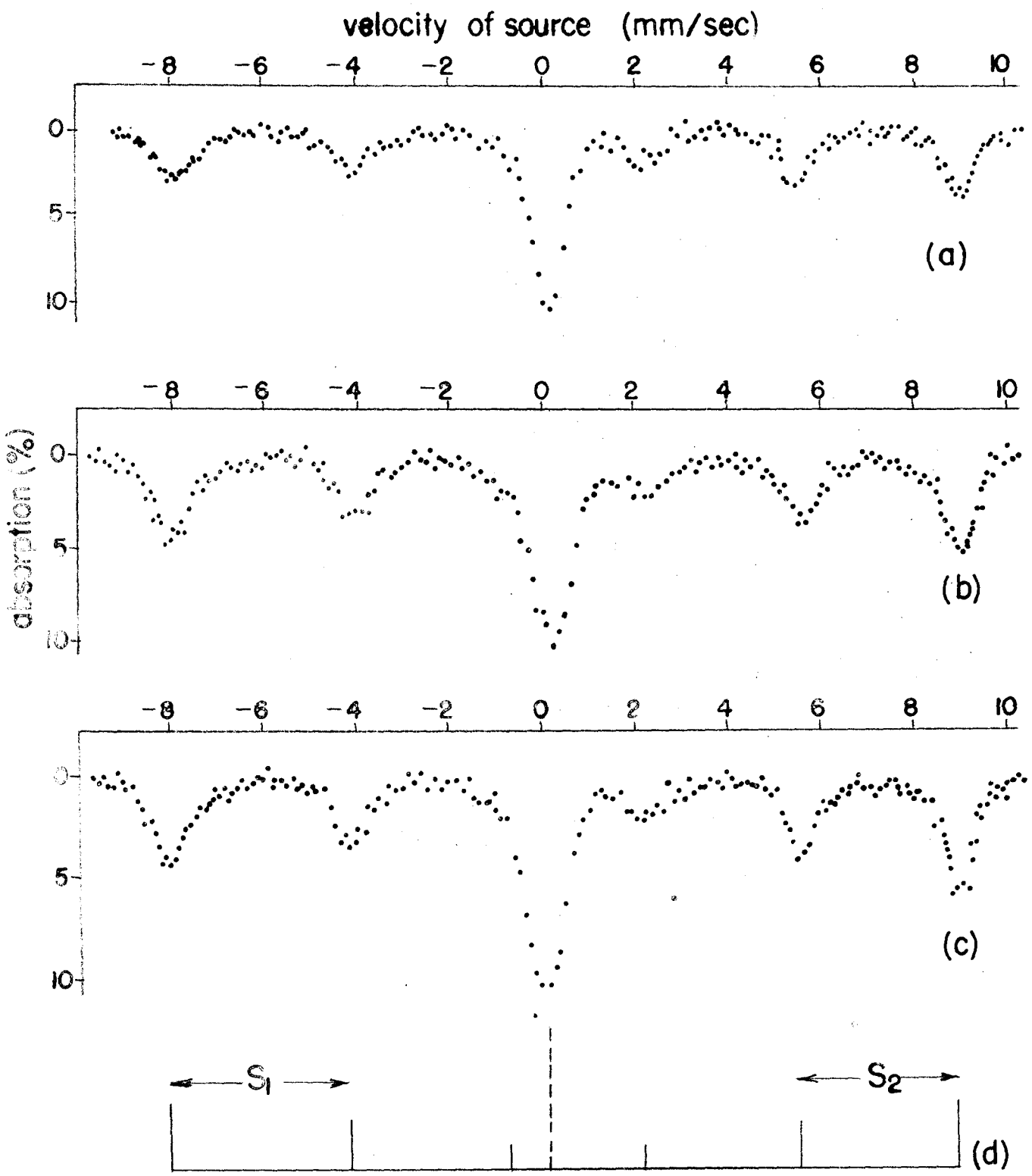
velocity of source (mm/sec)
-8 -6 -4 -2 0 2 4 6 8 10
0
5
10
absorption (%)
(a)
(b)
(c)
S1
S2
(d)

FIG. 11

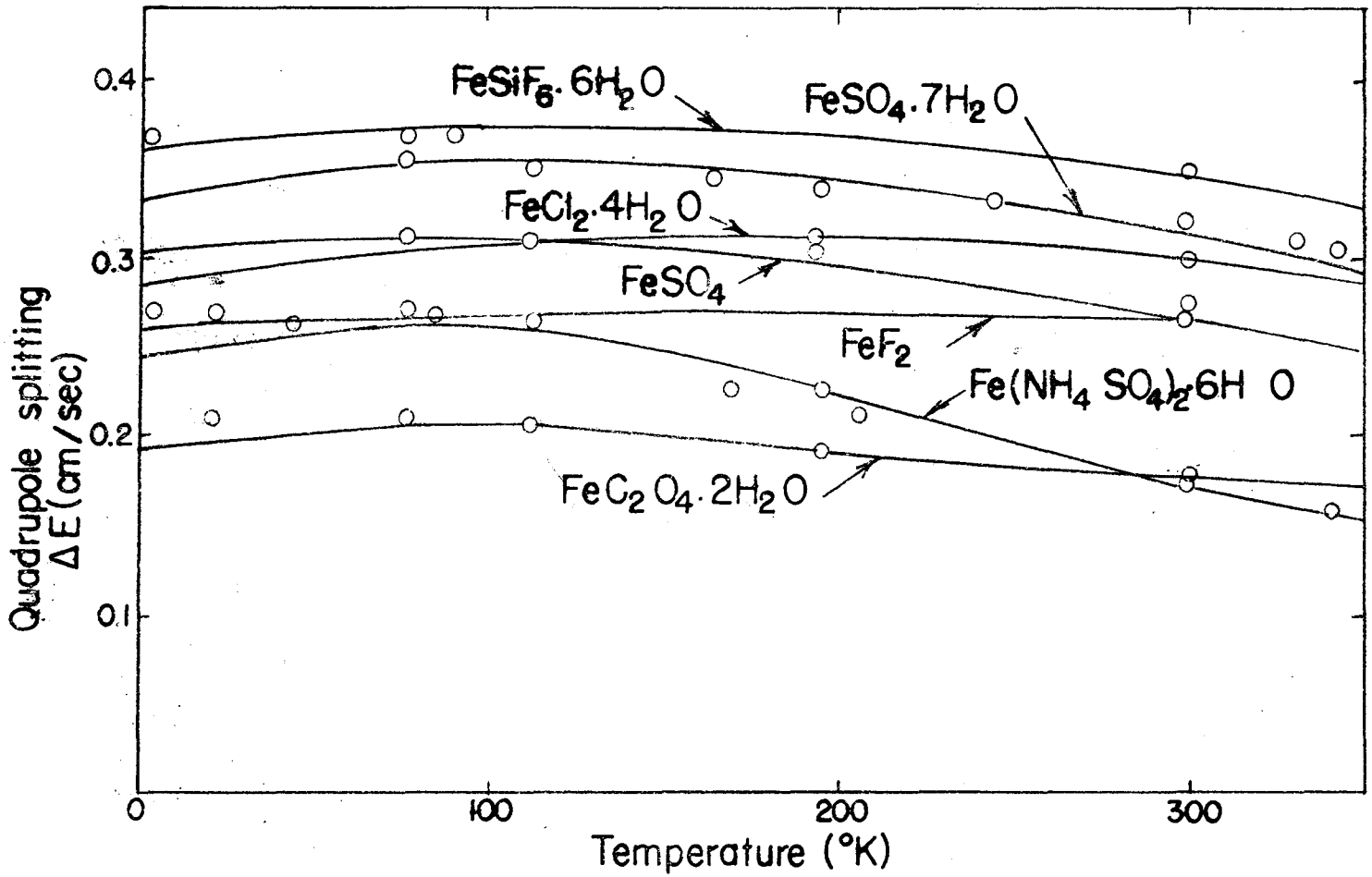
$FeSiF_6 \cdot 6H_2O$
$FeSO_4 \cdot 7H_2O$
$FeCl_2 \cdot 4H_2O$
$FeSO_4$
FeF_2
$Fe(NH_4SO_4)_2 6H_2O$
$FeC_2O_4 \cdot 2H_2O$
Quadrupole splitting
ΔE (cm/sec)
0.4
0.3
0.2
0.1
0
100
200
300
Temperature (°K)

FIG. 12

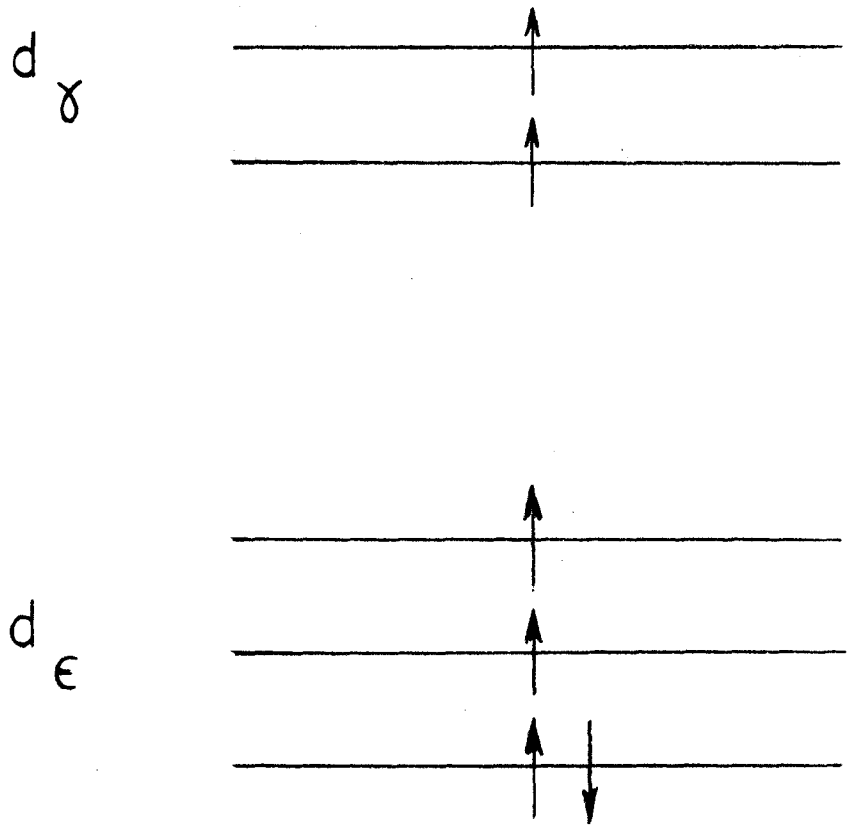

FIG. 13

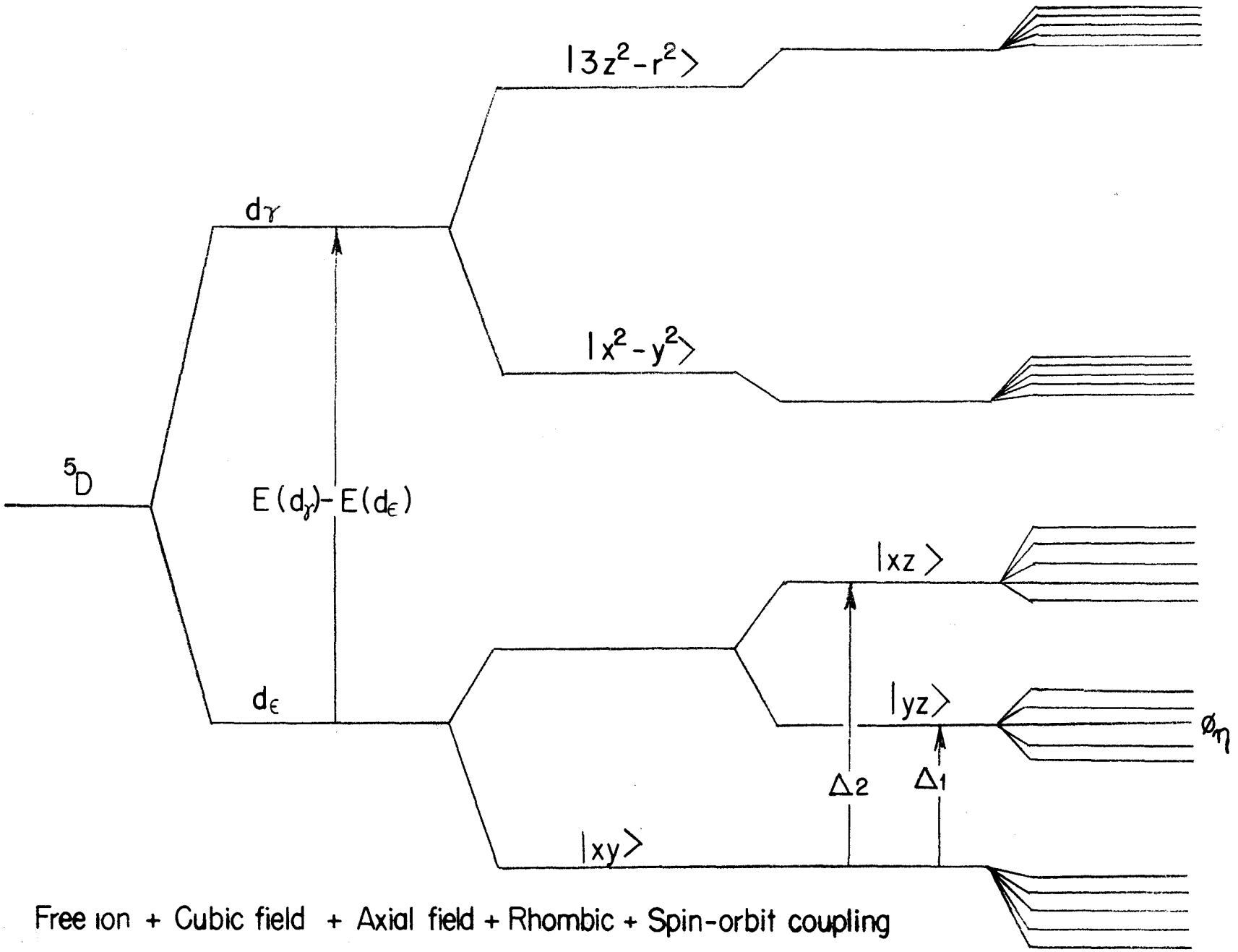
$|3z^2-r^2\rangle$
$d\gamma$
$|x^2-y^2\rangle$
^5D
$E(d_\gamma)-E(d_\epsilon)$
$|xz\rangle$
$d\epsilon$
$|yz\rangle$
ϕ_η
$\Delta 2$
$\Delta 1$
$|xy\rangle$
Free ion + Cubic field + Axial field + Rhombic + Spin-orbit coupling

FIG. 14

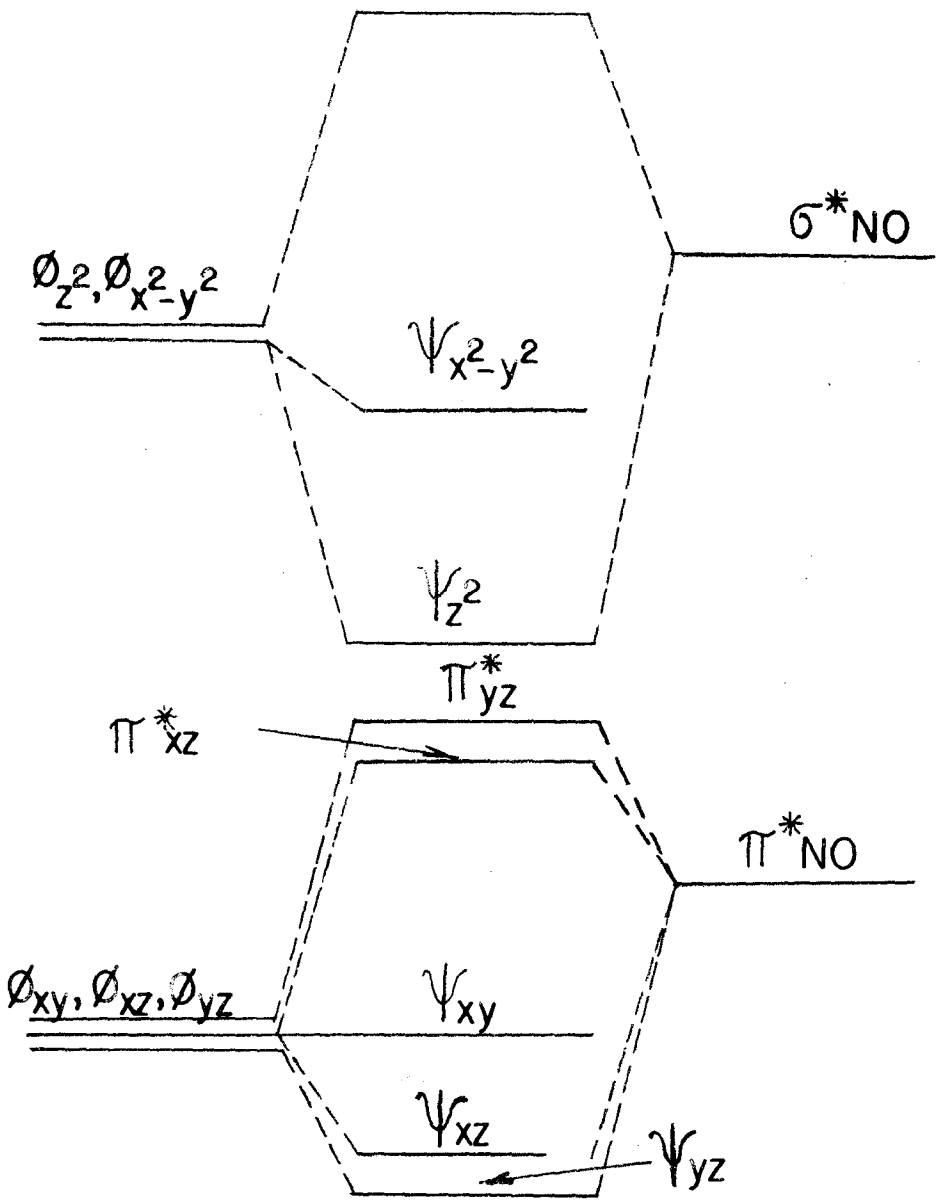

FIG. 15

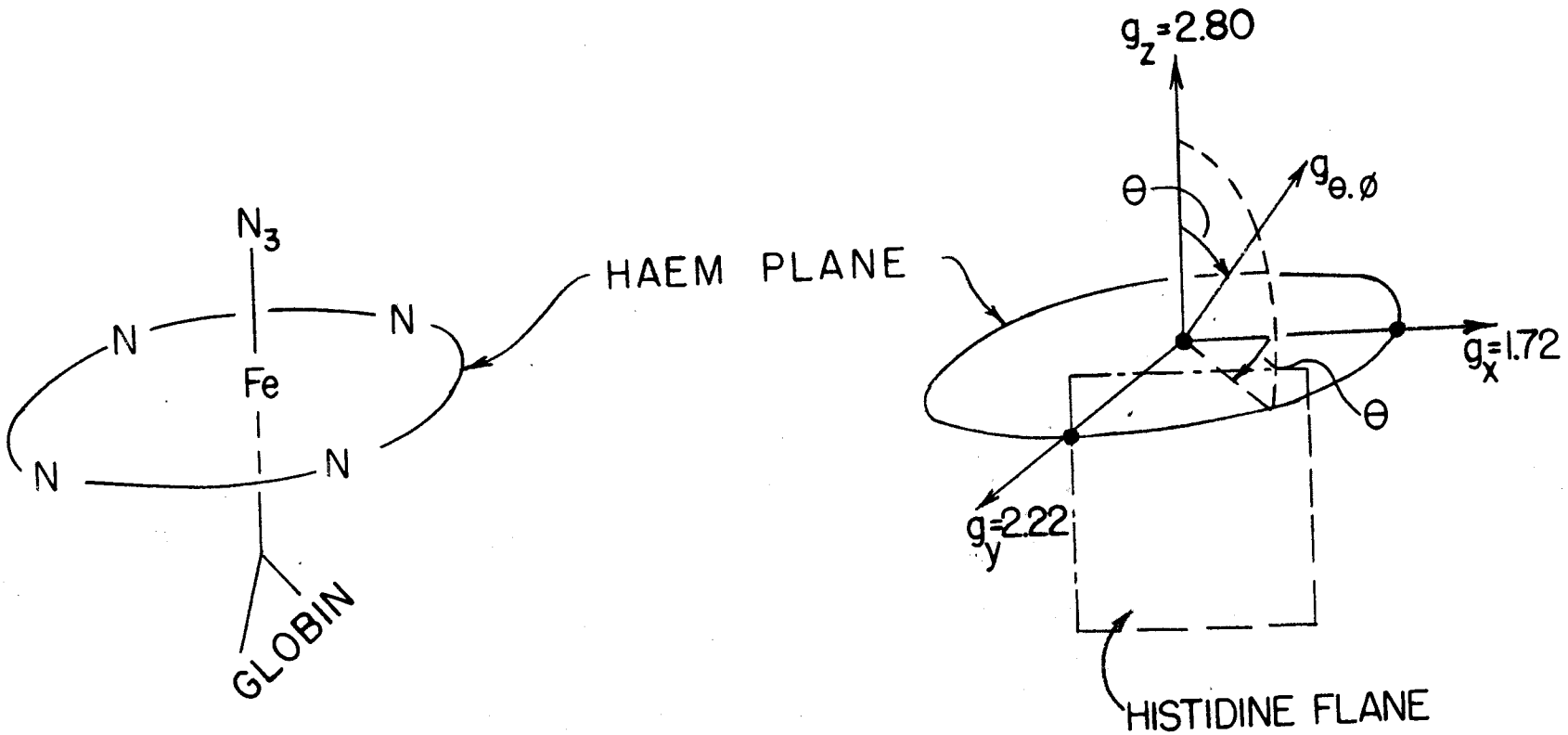

THE THREE PRINCIPAL AXES OF G-VALUE VARIATION FOR MYOGLOBIN AND HAEMOGLOBIN AZIDE

FIG. 16

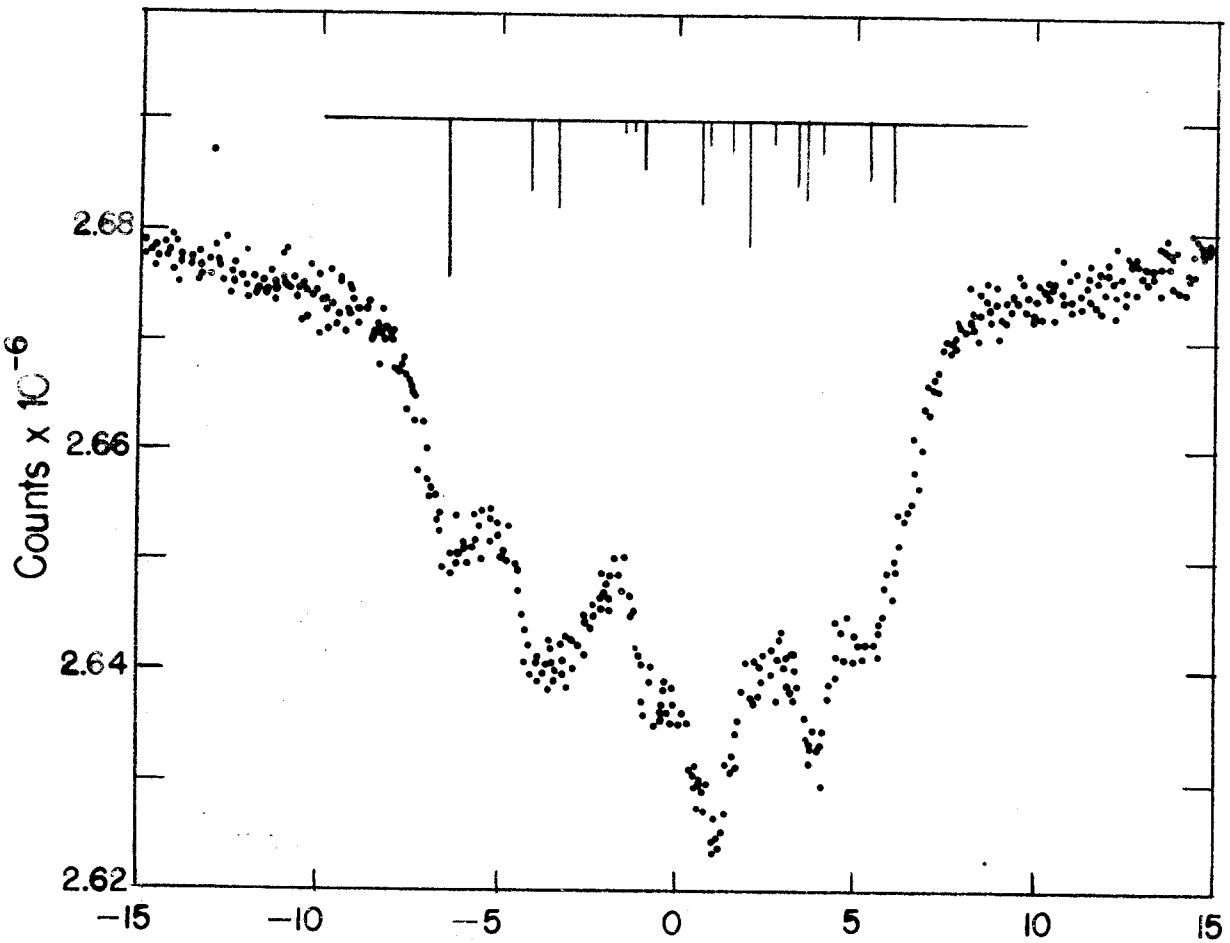

FIG. 17

REFERENCES:

1. Chemical Applications of Mössbauer Spectroscopy, Ed. V. I. Goldanskii and R. H. Herber - Academic Press, New York and London 1968.

2. J. Danon, Lectures on the Mössbauer Effect, Gordon and Breach, New York 1968.

3. N. N. Greenwood, Chemistry in Britain 3, 56 (1967).

4. J. Danon in "Physical Methods in Advanced Inorganic Chemistry", Ed. H. A. O. Hill and P. Day, Interscience Publishers, London 1969.

5. F. Albert Cotton and Geoffrey Wilkinson, Advanced Inorganic Chemistry, Interscience Publishers, New York 1966.

6. G. Kaindl, N. Petzel, F. Wagner, Ursel Zahn and R. L. Mössbauer - personal communication 1969.

7. G. R. Hoy and F. de S. Barros - Phys. Rev. 139, A 929 (1965).

8. J. Danon, Rev. Mod. Phys. 36, 454 (1964).

9. M. D. Lind, J. Chem. Phys. 46, 2010 (1967).

10. M. D. Lind, J. Chem. Phys. 47, 990 (1967).

11. Roger R. Berrett and Brian W. Fitzsimmons, J. Chem. Soc. (A), 525 (1967).

12. D. B. Brown, D. F. Shriever and L. H. Schwartz - Inorg. Chem. 7, 77 (1968).

13. E. Konig and K. Madeja, Chem. Comm. 61, (1966).

14. A. Ito, M. Suenaga and K. Ono - Technical Report ISSP, Ser. A, Nº 289, 1967; H. Chem. Phys. 48, 3597 (1968).

15. R. L. Ingalls - Phys. Rev. 133, A787 (1964).

16. J. Danon and L. Iannarella, J. Chem. Phys. 47, 382 (1967).

17. P. T. Manahoran and H. B. Gray, J. Am. Chem. Soc. 87, 3340 (1965).

18. A. Abragam and M. H. L. Pryce, Proc. Roy. Soc. (London) Ser. A. 205, 135 (1951).

19. J. S. Griffith, The Theory of Transition Metal Ions, Cambridge University Press, 1961.

20. G. Lang and W. Marshall, Proc. Phys. Soc. 87, 3 (1966).

21. G. Lang and W. Marshall in Mössbauer Effect Methodology, Ed. I. J. Gruverman, vol. 2, Plemim Press, New York 1966.

22. J. F. Gibson and D. J. E. Ingram, Nature 180, 29 (1967).

23. J. S. Griffith, Nature 180, 31 (1957).

* * *